Research Article

JPIS Journal of Periodontal & Implant Science

J Periodontal Implant Sci 2010;40:180-187 • doi: 10.5051/jpis.2010.40.4.180

Spontaneous healing capacity of rabbit cranial defects of various sizes

Joo-Yeon Sohn, Jung-Chul Park, Yoo-Jung Um, Ui-Won Jung, Chang-Sung Kim, Kyoo-Sung Cho, Seong-Ho Choi*

Department of Periodontology, Research Institute for Periodontal Regeneration, Yonsei University College of Dentistry, Seoul, Korea

Purpose: This study evaluated the spontaneous healing capacity of surgically produced cranial defects in rabbits with different healing periods in order to determine the critical size defect (CSD) of the rabbit cranium.

Methods: Thirty-two New Zealand white rabbits were used in this study. Defects of three sizes (6, 8, and 11 mm) were created in each of 16 randomly selected rabbits, and 15-mm defects were created individually in another 16 rabbits. The defects were analyzed using radiography, histologic analysis, and histometric analysis after the animal was sacrificed at 2, 4, 8, or 12 weeks postoperatively. Four samples were analyzed for each size of defect and each healing period.

Results: The radiographic findings indicated that defect filling gradually increased over time and that smaller defects were covered with a greater amount of radiopaque substance. Bony islands were observed at 8 weeks at the center of the defect in both histologic sections and radiographs. Histometrical values show that it was impossible to determine the precise CSD of the rabbit cranium. However, the innate healing capacity that originates from the defect margin was found to be constant regardless of the defect size.

Conclusions: The results obtained for the spontaneous healing capacity of rabbit cranial defects over time and the underlying factors may provide useful guidelines for the development of a rabbit cranial model for in vivo investigations of new bone materials.

Keywords: Experimental design, Osseous defect, Wound healing.

INTRODUCTION

The critical size defect (CSD) has been defined as the smallest intraosseous wound in an animal that will not heal spontaneously when left untreated for a certain time period [1] or which shows less than 10% bone regeneration during the lifetime of the animal [2]. The CSD has been used as an experimental model for evaluating the effectiveness of newly developed biomaterials [3].

There are several bone defect models, including those for the tibia, radius, mandible, and cranium. Among them, a cranial defect provides a model for non-load-bearing bone with relative biological inertness due to its poor blood supply and limited bone marrow, thereby resembling human mandibular bone [4]. Thus, cranial defects in validated small-animal models have been used in numerous studies for evaluating newly developed biomaterials for implantations prior to performing large-animal implantations [5].

The rabbit is commonly used in animal experiments for medical research. Some of its advantages are that it is easily handled, has a rapid bone turnover rate, and is fully mature within 6 months [6]. Rabbit cranial defects provide a good first

Received: May. 3, 2010; **Accepted:** Jul. 13, 2010

***Correspondence:** Seong-Ho Choi

Department of Periodontology, Research Institute for Periodontal Regeneration, Yonsei University College of Dentistry, 134 Sinchon-dong, Seodaemun-gu, Seoul 120-752, Korea

E-mail: shchoi726@yuhs.ac, Tel: +82-2-2228-3189, Fax: +82-2-392-0398

pISSN 2093-2278
eISSN 2093-2286

phase bone model for experiments related to bone graft materials and evaluations of bone regeneration due to the adequate amount of bone marrow facilitating bone formation [7,8]. Moreover, the rabbit has a larger cranium than the rat, which makes it possible to create multiple defects in one cranium, which reduces the operation time, cost, and observational errors among individuals. The effects of the size and shape of rabbit cranial defects on bone and membrane materials have been reported. Some researchers have evaluated bone regeneration of rectangular (10×10 mm) cranial defects, which were used as CSDs [9,10], and 10-mm circular defects [11]. In addition, 8- and 6-mm circular defects have generally been used when observing the effects of barrier membranes and bone graft materials [12-15]. Circular 15-mm defects also have been used as the CSD for investigating growth factors and graft materials [16-18].

However, few studies have analyzed the healing capacity histometrically in defects of different sizes over time. Whilst the CSD of the rabbit cranium has been investigated previously [4,13], its size and shape have not been standardized. Therefore, the purpose of this study was to measure the spontaneous healing capacity of surgically produced cranial defects in rabbits at different healing periods in order to determine the CSD of the rabbit cranium. Information obtained from this

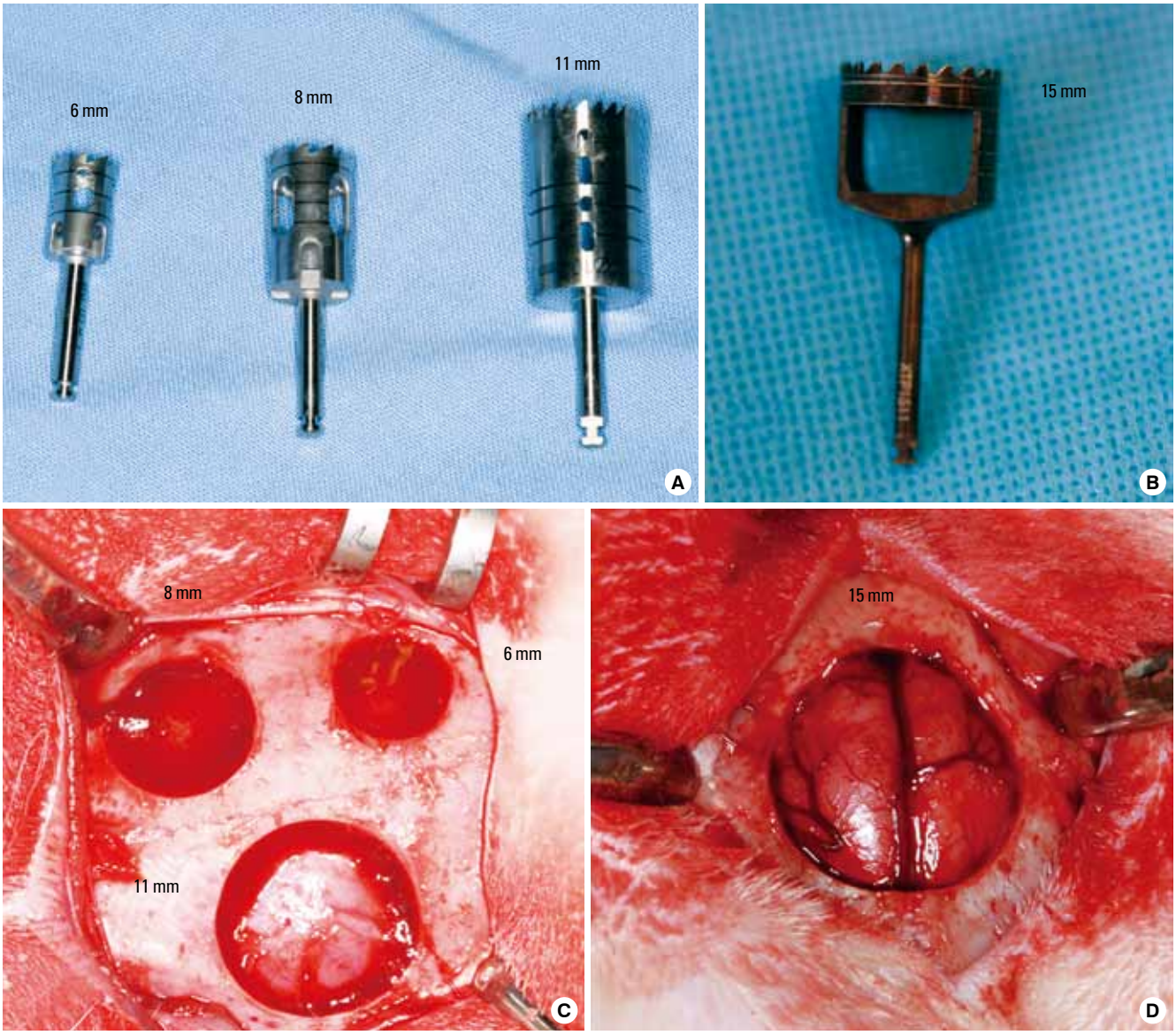

Figure 1. Trephine burs and different sizes of defects (A) The trephines with outer diameters of 6, 8, and 11 mm. (B) The trephine with an outer diameter of 15 mm. (C) Photograph of three standardized circular defects created with diameters of 6, 8, and 11 mm. (D) Photograph of a 15-mm defect, which includes a portion of the sagittal suturing.

JPIS Journal of Periodontal & Implant Science

study will be useful for making presurgical decisions related to the size and healing period of rabbit cranial defects.

MATERIALS AND METHODS

Animals

Thirty-two New Zealand white rabbits weighing 3.0-3.5 kg were used in this study. Defects of three sizes (6, 8, and 11 mm) were created in 16 randomly chosen rabbits, and 15-mm defects were created individually in the other 16 rabbits. The defects were analyzed after sacrificing the animals at 2, 4, 8, or 12 weeks postoperatively. Four samples were analyzed for each size of defect and each healing period.

The animals were housed in separate cages under standard laboratory conditions and fed a standard diet. Animal selection, management, surgical protocol, and preparation followed routines approved by the Institutional Animal Care and Use Committee, Yonsei Medical Center, Seoul, Korea (certification #08-267).

Surgical procedure

The animals were anesthetized with an intramuscular injection of a mixture of ketamine hydrochloride (Ketalar, Yuhan Co., Seoul, Korea) and xylazine (Rompun, Bayer Korea Co., Seoul, Korea). The surgical sites were shaven and then draped with alcohol and povidone iodine, followed by local anesthesia with 2% lidocaine (Lidocaine HCl, Huons, Seoul, Korea). An incision was made along the sagittal midline from the frontal bone to the occipital bone. A full-thickness flap was elevated to expose the cranial bone. Standardized circular defects with diameters of 6, 8, 11, and 15 mm were created using trephines of the corresponding sizes under cool-saline irrigation. The soft tissues were repositioned and then sutured layer by layer with a resorbable suture material (4-0 Vicryl, Ethicon, Somerville, NJ, USA) to achieve primary closure. The stitches were removed after 10 days. The animals were sacrificed at 2, 4, 8, or 12 weeks postoperatively (Fig. 1).

Evaluation

Postoperative management included the subcutaneous administration of antibiotics (Baytril, Bayer, Leverkusen, Germany) and the careful clinical observation of the animals throughout the healing period.

The area of the original surgical defect and surrounding tissues were removed en bloc after sacrifice. The sections were rinsed in sterile saline and fixed in 10% buffered formalin for 10 days. After rinsing in water, all specimens were radiographed using an X-ray machine (Diox, DigiMed, Seoul, Korea) before processing for the production of histologic slides. The extent of the defects' closure and newly formed radiopaque area was observed. The sections were decalcified in 5% formic acid for 14 days and embedded in paraffin. Serial sections were cut from the center at intervals of 5 μm. The most-central sections from each block were stained with hematoxylin and eosin (H&E) and examined using light microscopy (Leica DM LB, Leica Microsystems, Wetzlar, Germany).

Histometric analysis

Histometric measurements were made using image-analysis software (Image-Pro Plus., Media Cybernetics, Silver Spring, MA, USA). The measurement parameters are defined in the schematic diagram in Fig. 2, from which the following histometric parameters were determined:

1) Defect closure (%) = (total new bone ingrowth, mm)/(original defect width, mm)×100 (%).

The original defect width was measured and was considered to represent 100% of the width to be analyzed.

2) New bone area ratio (%) = (newly formed bone area, mm^2)/(total area, mm^2)×100 (%).

The total area was determined by first identifying the external and internal surfaces of the original cranium at the right and left margins of the surgical defect, and then connecting them with lines drawn by extrapolating from their respective curvatures. This method was partly based on the work of Melo et al. [19]. The total area was taken as 100% of the area to be analyzed.

3) New bone ingrowth (mm) = (sum of new bone ingrowth, mm)/2.

The average length of the new bone was measured from the right and left margins of the defect.

4) New bone area (mm^2).

The newly formed bone area was measured in mm^2.

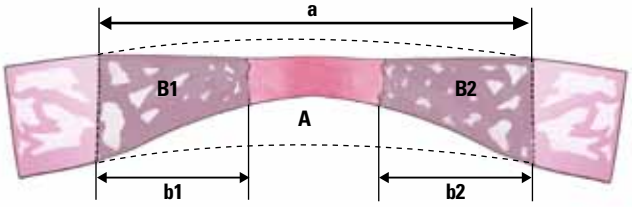

Figure 2. Schematic diagram of a calvarial osteotomy defect showing the measurement parameters from which the following histometric parameters were determined (with linear and area measurements in millimeters and millimeters squared, respectively): defect closure (%): (b1+b2)/a×100, new bone area ratio (%): (B1+B2)/A×100, new bone ingrowth (mm): (b1+b2)/2, new bone area (mm^2): B1+B2 where A represents the area within the dotted lines, corresponding to the total defect area; B1+B2 is the new bone area; and a, b1, and b2 represent the total defect width and the new bone ingrowth from the left and right margins, respectively.

Statistical analysis

The defect closure, new bone area ratio, new bone ingrowth, and new bone area for each healing period are expressed as mean and standard-deviation values. Data were analyzed using SPSS ver. 14.0 (SPSS Inc., Chicago, IL, USA). The significance of differences between groups with different defect sizes in relation to all of the histometric parameters were determined by the Kruskal-Wallis test followed by the Bonferroni test. The Kruskal-Wallis test was also used for comparisons between healing intervals within a single group. Statistical significance was determined at the $P<0.05$ level.

RESULTS

All animals tolerated the surgical procedures well, and the clinical healing process was generally uneventful, with there being no dehiscence of the surgical wound, signs of inflammation, or other complications.

Radiographic evaluation

A definite defect margin was observed with a small amount of radiopacity visible along the lateral margin in all specimens at 2 weeks. At 4 weeks the defect margin was partially obscured and there were irregular and asymmetric radiopaque areas at 1.0-1.5 mm from the defect margin. The defect margins could not be distinguished and the radiopaque area extended moderately inwards for a uniform distance at 8 weeks. Some bony islets that were separated from the marginal bone were evident in the central area of the defect.

At 12 weeks the 6-mm defects were almost filled with radiopaque substance except in the central portion. In some samples a bony bridge had formed from the marginal bone to the center, and the defect margin was no longer defined on the other diameters of the defects. The radiopaque substance extended inwards at 2.5-3.0 mm from all aspects of the margin (Fig. 3).

Histologic evaluation

A small amount of wedge-shaped bone had regenerated at 2 weeks. Most of the newly formed bone was woven bone, which showed limited bone marrow and a large number of osteoclasts. Bone regeneration was slightly greater at 4 weeks than at 2 weeks, and moderate amounts of bone regeneration and bone marrow began to appear. Active new bone forma-

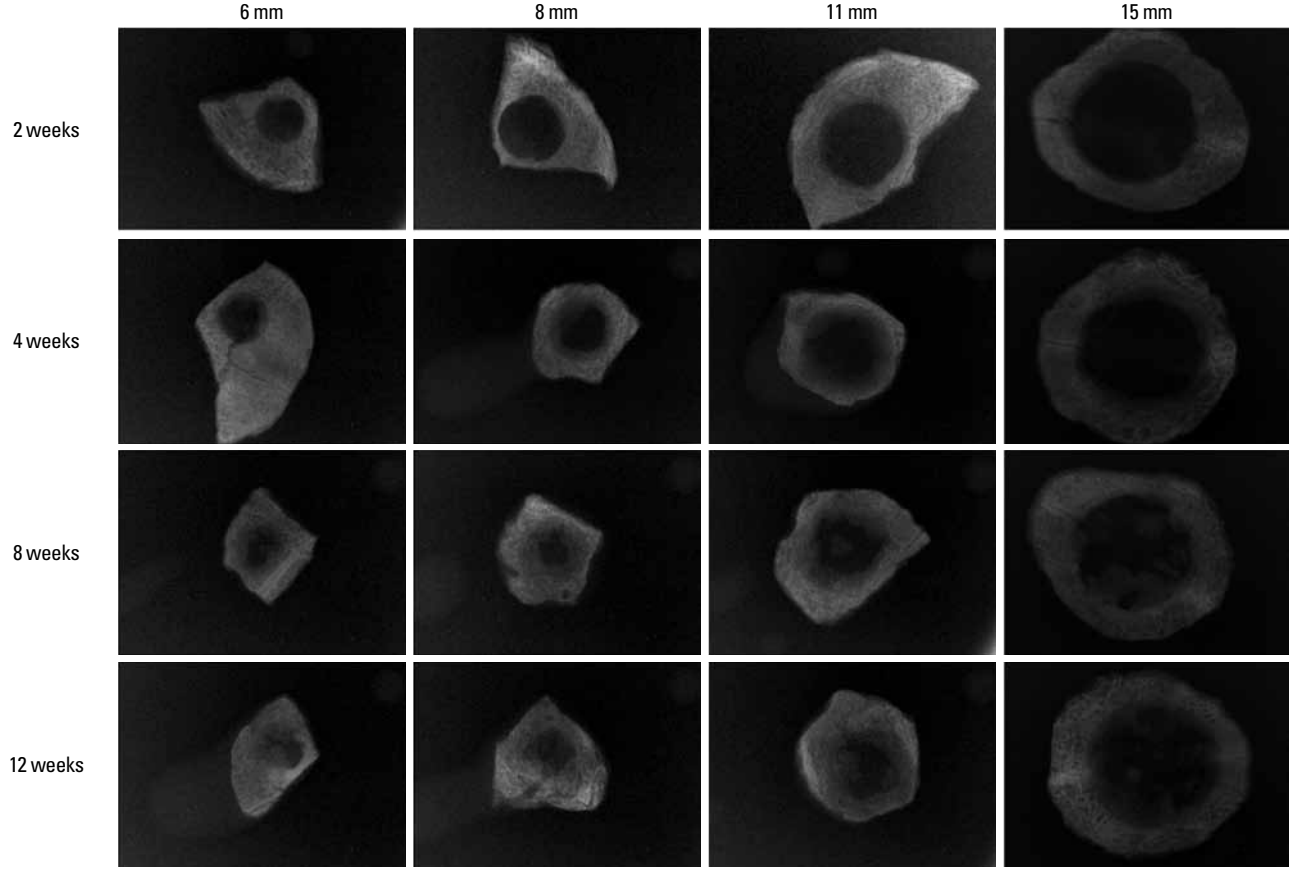

Figure 3. Radiographic views of the surgical defects at different healing periods.

JPIS Journal of Periodontal & Implant Science

tion was also present, with osteoid seams lined by plump osteoblasts.

At 8 weeks the newly formed bone had a moderate amount of bone marrow and had matured. Bone regeneration from the margin was markedly increased in both width and length. Bony islands that appeared in some specimens on the center of the defects contained moderate amounts of bone marrow. Lamellar bone was formed in the newly formed bone at 12 weeks, even in the bony islets. A bone bridge was evident in some of the specimens with 6-mm defects (Fig. 4).

Histometric analysis

The defect closure and new bone area ratio at postoperative weeks 2, 4, 8, and 12 are listed in Table 1. The defect closure differed significantly between the 15-mm-defect group and the 6- and 8-mm-defect groups at 2 and 4 weeks after the surgery: It was 88.57±4.52% and 50.15±17.99% in the 6- and 15-mm-defect groups, respectively, at 12 weeks after the surgery. However, the defect closure did not vary significantly with the defect size at 8 weeks.

The mean new bone area ratios at 12 weeks were 53.59%, 41.82%, 35.06%, and 20.13% in the 6-, 8-, 11-, and 15-mm-defect groups, respectively. The new bone area ratio differed significantly between the 15-mm-defect group and the 6- and 8-mm-defect groups at all healing periods.

The values of the measurement parameters gradually increased over time. However, the defect closure and the new bone area ratio did not differ significantly between weeks 2 and 4 or between weeks 8 and 12 except in the 6-mm-defect group, which showed a significant difference between 8 and 12 weeks.

Table 2 lists the values of new bone ingrowth from the margin and new bone area, respectively. The new bone ingrowth gradually increased with the healing period, ranging from 1.30 to 1.59 mm at 2 weeks and from 2.57 to 3.00 mm at 12 weeks. However, neither the new bone ingrowth nor the new bone area differed significantly between the groups at the same healing period.

Table 1. Mean±SD values of the DC and the NBR as percentages within surgically created defects (n=4).

DC (%)	2 weeks	4 weeks	8 weeks	12 weeks
6 mm	43.31±9.18[a,c,d]	47.39±7.31[a,c]	66.06±12.62[c]	88.57±4.52[a]
8 mm	40.80±9.27[a,c]	44.38±5.37[a,c]	65.35±9.58	78.70±17.65
11 mm	28.67±4.51[c]	36.96±6.72	50.03±25.92	66.89±19.65
15 mm	14.98±3.55[c,d]	27.67±7.24	40.83±5.85	50.15±17.99
NBR (%)	**2 weeks**	**4 weeks**	**8 weeks**	**12 weeks**
6 mm	25.59±8.18[a,c,d]	32.32±4.01[a,c,d]	47.18±6.87[a,b]	53.59±6.67[a,b]
8 mm	22.50±5.23[a,c,d]	28.15±3.95[a,c,d]	39.21±3.11[a]	41.82±5.72[a]
11 mm	17.07±3.64[c]	25.63±6.13[a]	27.57±10.61	35.06±8.33
15 mm	5.54±2.83[c,d]	12.11±2.81	19.70±2.57	20.13±5.90

DC: defect closure, NBR: new bone area ratio.
[a]Statistically significant difference from the 15-mm-defect group at the same healing period ($P<0.05$).
[b]Statistically significant difference from the 11-mm-defect group at the same healing period ($P<0.05$).
[c]Statistically significant difference from the 12-week healing period in the same size defect group ($P<0.05$).
[d]Statistically significant difference from the 8-week healing period in the same size defect group ($P<0.05$).

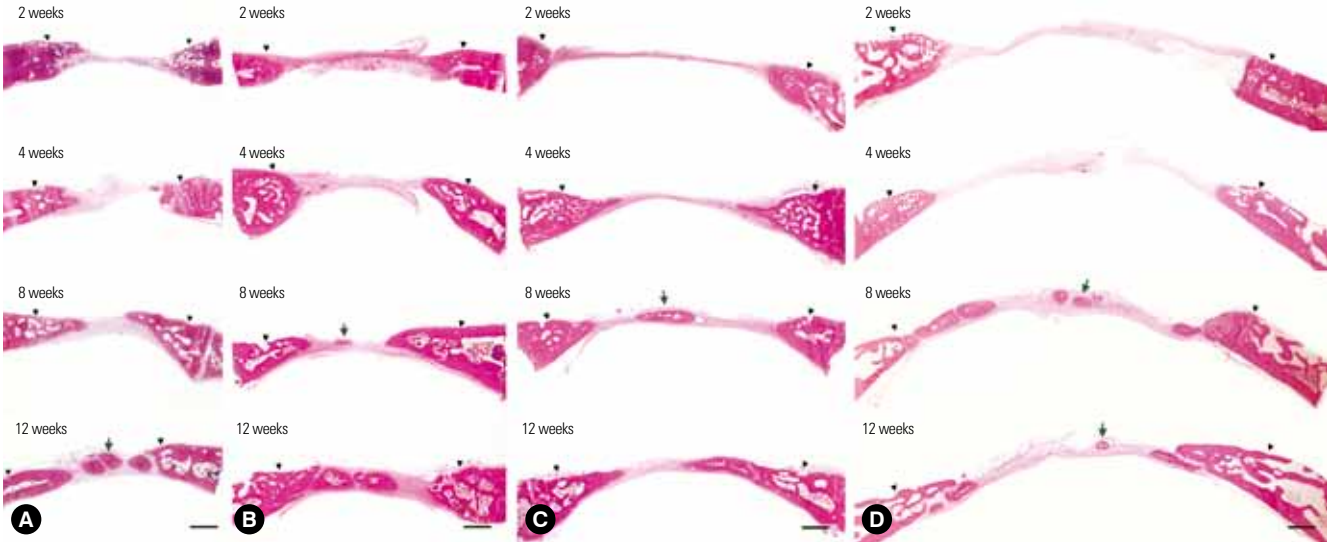

Figure 4. Histologic views of the surgical defects at different healing periods (H&E stain, ×10). Arrowheads point to the original defect margins, and the arrows show bony islets. The scale bar indicates 10 mm. Defect sizes: (A) 6 mm, (B) 8 mm, (C) 11 mm, and (D) 15 mm.

Table 2. Mean±SD values of the extent of new bone ingrowth (in millimeters) and the new bone area (in millimeters squared) within surgically created defects (n=4).

New bone ingrowth	2 weeks	4 weeks	8 weeks	12 weeks
6 mm	1.46±0.28	1.55±0.50	1.98±0.41	2.57±0.20
8 mm	1.59±0.39	1.69±0.12	2.41±0.32	2.74±0.29
11 mm	1.57±0.25	1.85±0.13	2.44±0.39	2.99±0.66
15 mm	1.30±0.26	1.77±0.26	2.30±0.34	3.00±0.58
New bone area	2 weeks	4 weeks	8 weeks	12 weeks
6 mm	1.53±0.58	1.78±0.57	2.70±0.66	3.20±0.31
8 mm	1.88±0.67	2.25±0.65	3.19±0.27	3.44±0.89
11 mm	2.27±0.67	2.75±0.93	3.88±0.96	4.03±0.69
15 mm	1.72±0.23	2.88±0.85	3.83±0.64	3.90±0.21

No significant difference among the groups at all healing periods ($P<0.05$).

DISCUSSION

Numerous bone graft materials have been developed and evaluated using defects created in the rabbit cranium with the aim of confirming their biologic stability and osteoinductive properties in clinical applications [11-14,20-22]. Investigations of the ability of bone graft materials to produce complete bone healing of a defect necessitate the use of a CSD to exclude spontaneous bony regeneration of the defect. Despite the importance of the CSD, precise analyses of spontaneous healing capacity have not been discussed in the literature, and different studies have considered CSDs in the range of 10-15 mm to be suitable [9,10,16-18]. The present study surgically created circular defects of 6, 8, 11, and 15 mm in the craniums of New Zealand White rabbits to evaluate their spontaneous healing capacity at different healing periods in order to determine the CSD.

Bone marrow began to mature and bony islets were observed after 8 weeks of healing. The defect closure and the new bone area ratio gradually increased with the healing time, but these parameters did not differ significantly between weeks 2 and 4 or between weeks 8 and 12. An observation period of at least 12 weeks was recommended by Bodde et al. [3] for evaluating bone formation in CSD models. Our results indicate that the healing period should be chosen according to the purpose of the experiments: A healing period of 2-4 weeks could be recommended for evaluating the early phase of the healing reponse, such as the stability of the materials or host reactions, while 8 weeks or more may be appropriate for assessing late healing, such as bone incorporation, resorption of materials, bone remodeling, or the amount of bone regeneration.

In the 15-mm defects, which have been previously used as a CSD for investigating bone regeneration in many studies [16-18], the defect closure and new bone area ratio were 50.15±17.99% and 20.13±5.90%, respectively, at 12 weeks. To fulfill the definition of the CSD, less than 10% of bone regeneration should be observed during the lifetime of the animal [2], and this period should encompass at least one complete bone-remodeling cycle. Although 15-mm defects failed to heal spontaneously at 12 weeks in the present study, they did not satisfy the definition of the CSD [2] since the percentage of new bone area exceeded 20%.

Many researchers have selected a defect smaller than the CSD for investigating the early events of regeneration or comparing various implant materials [23-25]. It is possible to create multiple defects in one animal when a small defect is used, which could allow for the experimental testing of all materials under investigation in single animals and thereby avoid individual variation. In the present study, the defect closure and new bone area did not differ significantly between the 11- and 15-mm-defect groups over the entire healing period. These findings indicate that it is possible to prepare two symmetric 11-mm defects in most rabbit craniums without involving sagittal suturing, which could be an alternative to creating one 15-mm defect, especially for evaluating the mid-phase or late-healing period. If several materials need to be compared only for early-phase healing, four 8-mm defects could be created in a single rabbit cranium.

The new bone ingrowth ranged from 1.19 to 1.69 mm at 2 weeks and from 2.41 to 3.62 mm at 12 weeks, and did not differ significantly between the groups at the same healing period; there was also no significant intergroup difference in the new bone area. These results indicate that the healing capacity from the defect margin is constant at the same healing period regardless of the defect size. If the defect is smaller than the new bone ingrowth at a certain time of healing, the defect will be covered and filled with the new bone, and bone union will be accomplished spontaneously. Thus, innate wound-healing potential could be one of the important factors determining the appropriate sizes of experimental defects and the healing period.

Some radiographs obtained in the present study showed bony islets in the central area of defects that were away from the defect edge. Vogeler et al. [26] reported differences in osteogenesis between central and peripheral new bone within cranial defects, and found that regeneration in cranial defects occurred both from the cut edges of the bone and from islands of bone within the dura mater and periosteum. The periosteum provides cortical bone with a blood supply [1,2], and the dura mater has been demonstrated to contribute to the reossification of cranial defects due to its osteogenic potential [27]. However, the dura mater can be easily damaged when creating defects, and hence the healing of cranial defects is usually accomplished from the defect edge and periosteum.

JPIS Journal of Periodontal & Implant Science

Huh et al. [28] showed that the CSD depends on the presence of the periosteum and considered it necessary to differentiate CSDs according to whether the periosteum is present. In the present study, the dura mater of the defect was gently removed with a pincette in all of the samples so as to ensure consistent conditions, and the periosteum was repositioned and sutured with a resorbable suture material to prevent ingrowth of the soft tissue into the defects. Bony islets separate from the defect margin appeared in some samples after 8 weeks of healing, which we considered to have originated from the periosteum. It is difficult to exclude factors such as the dura mater and periosteum completely in bone regeneration, and hence healing should be evaluated separately at the margin and central area at a certain healing period whilst considering these factors. Moreover, determining the precise CSD for the rabbit cranium will require additional experiments in which the defects are created without periosteum.

The results of the present study suggest that the CSD is larger than 15 mm, but it would be impossible to create such large defects in a single rabbit cranium. An 11-mm defect is therefore a good alternative option, since we found that none of the measurement parameters differed significantly between 11- and 15-mm defects throughout the healing period. Two 11-mm defects can be created in a single cranium without involving a sagittal suture line, thereby reducing the cost and the errors between individuals. Moreover, four 8-mm defects could be used to investigate the early-phase healing response and to simultaneously compare several materials whilst avoiding individual variation.

To evaluate the early phase of the healing response, such as the stability of the materials or the host reaction, a healing period of 2-4 weeks could be recommended. Eight weeks or more could be used to assess late healing, such as bone incorporation, resorption of materials, bone remodeling, or the amount of bone regeneration. Moreover, since the bony islets away from the defect margin would be formed in the center of the defect after 8 weeks, bone regeneration of the central area should be evaluated separately.

The innate healing capacity that originates from the defect margin is constant regardless of the defect size. Therefore, the innate healing capacity should be considered when choosing the healing period and the defect size. In addition, when determining the appropriate experimental method, the management of the dura mater and periosteum should be unified in order to obtain consistent and accurate results.

The present study investigated the spontaneous healing capacity of rabbit cranial defects over time and underlying factors. Within the limitations of this study, the obtained results may provide useful guidelines for the development of a rabbit cranial model for in vivo investigations of new bone materials.

CONFLICT OF INTEREST

No potential conflict of interest relevant to this article was reported.

ACKNOWLEDGMENTS

This research was supported by the Basic Science Research Program through the National Research Foundation of Korea (NRF) funded by the Ministry of Education, Science and Technology (R13-2003-013-04002-0).The authors wish to thank Dr. Je-Young Yon for his expertise in conducting the statistical analysis and Mr. Jin-Woo Lee for the schematic description.

REFERENCES

1. Bos GD, Goldberg VM, Powell AE, Heiple KG, Zika JM. The effect of histocompatibility matching on canine frozen bone allografts. J Bone Joint Surg Am 1983;65:89-96.
2. Schmitz JP, Hollinger JO. The critical size defect as an experimental model for craniomandibulofacial nonunions. Clin Orthop Relat Res 1986;205:299-308.
3. Bodde EW, Spauwen PH, Mikos AG, Jansen JA. Closing capacity of segmental radius defects in rabbits. J Biomed Mater Res A 2008;85:206-17.
4. Frame JW. A convenient animal model for testing bone substitute materials. J Oral Surg 1980;38:176-80.
5. Le Guehennec L, Goyenvalle E, Aguado E, Houchmand-Cuny M, Enkel B, Pilet P, et al. Small-animal models for testing macroporous ceramic bone substitutes. J Biomed Mater Res B Appl Biomater 2005;72:69-78.
6. Gilsanz V, Roe TF, Gibbens DT, Schulz EE, Carlson ME, Gonzalez O, et al. Effect of sex steroids on peak bone density of growing rabbits. Am J Physiol 1988;255:E416-21.
7. Newman E, Turner AS, Wark JD. The potential of sheep for the study of osteopenia: current status and comparison with other animal models. Bone 1995;16:277S-84S.
8. Castaneda S, Largo R, Calvo E, Rodriguez-Salvanes F, Marcos ME, Diaz-Curiel M, et al. Bone mineral measurements of subchondral and trabecular bone in healthy and osteoporotic rabbits. Skeletal Radiol 2006;35:34-41.
9. Pripatnanont P, Nuntanaranont T, Vongvatcharanon S. Proportion of deproteinized bovine bone and autogenous bone affects bone formation in the treatment of calvarial defects in rabbits. Int J Oral Maxillofac Surg 2009;38:356-62.
10. Gosain AK, Santoro TD, Song LS, Capel CC, Sudhakar PV, Matloub HS. Osteogenesis in calvarial defects: contribu-

tion of the dura, the pericranium, and the surrounding bone in adult versus infant animals. Plast Reconstr Surg 2003;112:515-27.
11. Xu S, Lin K, Wang Z, Chang J, Wang L, Lu J, et al. Reconstruction of calvarial defect of rabbits using porous calcium silicate bioactive ceramics. Biomaterials 2008;29:2588-96.
12. Hammerle CH, Schmid J, Olah AJ, Lang NP. Osseous healing of experimentally created defects in the calvaria of rabbits using guided bone regeneration. A pilot study. Clin Oral Implants Res 1992;3:144-7.
13. Kramer IR, Killey HC, Wright HC. A histological and radiological comparison of the healing of defects in the rabbit calvarium with and without implanted heterogeneous anorganic bone. Arch Oral Biol 1968;13:1095-106.
14. Lundgren D, Nyman S, Mathisen T, Isaksson S, Klinge B. Guided bone regeneration of cranial defects, using biodegradable barriers: an experimental pilot study in the rabbit. J Craniomaxillofac Surg 1992;20:257-60.
15. Pallesen L, Schou S, Aaboe M, Hjorting-Hansen E, Nattestad A, Melsen F. Influence of particle size of autogenous bone grafts on the early stages of bone regeneration: a histologic and stereologic study in rabbit calvarium. Int J Oral Maxillofac Implants 2002;17:498-506.
16. Shand JM, Heggie AA, Holmes AD, Holmes W. Allogeneic bone grafting of calvarial defects: an experimental study in the rabbit. Int J Oral Maxillofac Surg 2002;31:525-31.
17. Cameron S. Hand-held computers in medicine. Can Fam Physician 2002;48:111-2.
18. Nagata MJ, Melo LG, Messora MR, Bomfim SR, Fucini SE, Garcia VG, et al. Effect of platelet-rich plasma on bone healing of autogenous bone grafts in critical-size defects. J Clin Periodontol 2009;36:775-83.
19. Melo LG, Nagata MJ, Bosco AF, Ribeiro LL, Leite CM. Bone healing in surgically created defects treated with either bioactive glass particles, a calcium sulfate barrier, or a combination of both materials. A histological and histometric study in rat tibias. Clin Oral Implants Res 2005;16:683-91.
20. Cavalcanti SC, Pereira CL, Mazzonetto R, de Moraes M, Moreira RW. Histological and histomorphometric analyses of calcium phosphate cement in rabbit calvaria. J Craniomaxillofac Surg 2008;36:354-9.
21. Durmus E, Celik I, Aydin MF, Yildirim G, Sur E. Evaluation of the biocompatibility and osteoproductive activity of ostrich eggshell powder in experimentally induced calvarial defects in rabbits. J Biomed Mater Res B Appl Biomater 2008;86:82-9.
22. Torres J, Tamimi FM, Tresguerres IF, Alkhraisat MH, Khraisat A, Lopez-Cabarcos E, et al. Effect of solely applied platelet-rich plasma on osseous regeneration compared to Bio-Oss: a morphometric and densitometric study on rabbit calvaria. Clin Implant Dent Relat Res 2008;10:106-12.
23. Glowacki J, Altobelli D, Mulliken JB. Fate of mineralized and demineralized osseous implants in cranial defects. Calcif Tissue Int 1981;33:71-6.
24. Strates BS, Connolly JF. Osteogenesis in cranial defects and diffusion chambers. Comparison in rabbits of bone matrix, marrow, and collagen implants. Acta Orthop Scand 1989;60:200-3.
25. Urist MR, Nilsson O, Rasmussen J, Hirota W, Lovell T, Schmalzreid T, et al. Bone regeneration under the influence of a bone morphogenetic protein (BMP) beta tricalcium phosphate (TCP) composite in skull trephine defects in dogs. Clin Orthop Relat Res 1987;214:295-304.
26. Vogeler KT, Redenz E, Walter H, Martin G, Deutsche Gesellschaft fur Chirurgie. Bernhard Heines Versuche uber Knochenregeneration: sein Leben und seine Zeit. Berlin: J. Springer; 1926.
27. Greenwald JA, Mehrara BJ, Spector JA, Chin GS, Steinbrech DS, Saadeh PB, et al. Biomolecular mechanisms of calvarial bone induction: immature versus mature dura mater. Plast Reconstr Surg 2000;105:1382-92.
28. Huh JY, Choi BH, Kim BY, Lee SH, Zhu SJ, Jung JH. Critical size defect in the canine mandible. Oral Surg Oral Med Oral Pathol Oral Radiol Endod 2005;100:296-301.